Dendrimer-Based Nanoplatforms for SPECT Imaging Applications

12

Lingzhou Zhao, Xiangyang Shi, and Jinhua Zhao

Contents

L. Zhao · J. Zhao (✉)
Department of Nuclear Medicine, Shanghai General Hospital, Shanghai Jiao Tong University School of Medicine, Shanghai, People's Republic of China
e-mail: zhaojinhua1963@126.com

X. Shi (✉)
College of Chemistry, Chemical Engineering and Biotechnology, Donghua University, Shanghai, People's Republic of China

CQM-Centro de Química da Madeira, Universidade da Madeira, Funchal, Portugal
e-mail: xshi@dhu.edu.cn

C. S. S. R. Kumar (ed.), *Nanotechnology Characterization Tools for Biosensing and Medical Diagnosis*, https://doi.org/10.1007/978-3-662-56333-5_12

1 Definition of the Topic

Dendrimers can be functionalized with multiple imaging and therapeutic moieties to establish dendrimer-based nanoplatforms for various applications. In this chapter we describe the recent progress in dendrimer-based nanomaterials for SPECT imaging applications with different purposes.

2 Overview

Dendrimers provide viable platforms for molecular imaging of organs and other target-specific diseases due to their unique and well-defined molecular architecture. Recent innovations in dendrimer nanotechnology have led to a rapid development of multi-functional radiolabeled nanoparticles for diagnosis and therapy of diseases. In this chapter, we review the recent advances in dendrimer-based nanosystems for SPECT imaging applications including single-mode SPECT imaging, dual-mode SPECT/CT, SPECT/MR, and SPECT/optical imaging and theranostics of cancer or other diseases.

3 Introduction

Precision becomes one of the core values in today's healthcare environment [1, 2]. Medical imaging, an essential technology in this context, providing precise imaging information, constantly deepens the understanding and instructs the treatment of many diseases [3–6]. During the last several decades, the number of imaging technologies and their applications in clinical practice have unprecedentedly increased. Currently, numerous imaging modalities are being used in biomedical and clinical settings for diagnostic and therapy purposes, including magnetic resonance (MR) imaging [7–11], computed tomography (CT) [12–16], positron emission tomography (PET) [17–19], single photon emission computed tomography (SPECT) [20, 21], and optical imaging [22, 23]. Among these, SPECT, PET, and optical imaging are known as functional imaging modalities, while CT and MRI are normally utilized to acquire anatomical information [24, 25].

Although each imaging modality is being continuously developed and improved for disease diagnosis, prognosis, or therapy monitoring, they are applied with intrinsic advantages and limitations [17, 26–28]. For example, optical imaging has a comparatively high sensitivity, whereas its absorption and scattering properties of tissue components limit the penetration depth to less than 10 mm [28]. PET and SPECT both are quantitative imaging techniques with high sensitivity and ability of observing physiological processes, but spatially limited in resolution [17]. MRI and CT are relatively insensitive imaging techniques but show operation convenience and extreme spatial resolution [26, 27]. Clearly, no single modality provides all of the required information. Hence, dual or multimode imaging approaches that combine functional and anatomic imaging into a single superposed image have emerged to integrate their advantages of

each imaging modality [29–31], and numerous efforts have been devoted to develop multimodality imaging techniques over the last decade [32–34]. Up to now, PET/CT and SPECT/CT with high fusion accuracy are the most successful paragons and have revolutionized medical diagnosis in many fields [35–37]. Lately, PET/MRI, a new diagnostic method with an excellent soft tissue contrast and less radiation dose than PET/CT, has been well developed and used for clinical imaging [38, 39]. These hybrid imaging techniques have gained wide acceptance as powerful tools in preclinical and clinical applications; however, few new imaging agents have been provided for multimodal hybrid imaging during the last decade. Therefore, a number of researchers are attempting to exploit versatile imaging platforms for early diagnosis, accurate prognosis, precision imaging, and image-guided drug delivery [40–42].

Recent progresses in nanotechnology have enabled the development of various advanced imaging agents. By virtue of the unique electrical, magnetic, and optical properties of nanomaterials, a variety of multifunctional nanosystems have been designed and manufactured as contrast agents for different imaging applications [42–45]. These nanosystems not only present enhanced contrast imaging effects, low toxicity, and prolonged circulation time but also possess active targeting ability by means of modification with targeting molecules. Among the developed nanomaterials, dendrimers have been praised as promising platforms to build multiple types of contrast agents due to their exquisite structures [46–48]. In this chapter, we will describe the use of dendrimer-based nanosystems for SPECT imaging including single-mode SPECT imaging, dual-mode SPECT/CT, SPECT/MR, and SPECT/optical imaging and theranostics of cancer or other diseases. To the best of our knowledge, this is the first review article specifically describing the progress of dendrimer-based SPECT agents and their applications in different aspects.

4 Experimental and Instrumental Methodology

4.1 Dendrimers

Dendrimers, a class of highly branched, monodispersed, synthetic macromolecules with well-defined architecture and composition, have highly controllable size and surface properties, which are quite different from linear polymers [49–51]. Dendrimers with nanometer-scale dimensions are composed of three components: a central core, a highly branched interior, and an exterior surface with functional groups. The unique features of dendrimers afford the varied combination of these components to form various functional nanoparticles (NPs) with different shapes, sizes, and modifications for materials sciences and biomedical applications [52]. Especially in the field of medical imaging, the plentiful terminal groups on the dendrimer periphery can be easily modified with multiple imaging moieties to provide dual-mode and multimode imaging functionalities within a single dendrimer molecule [46–48]. Similarly, the generation-dependent physical size of dendrimers may be used to tune their excretion behavior and imaging time, to optimize the payloads of different imaging elements, and to adjust the passive targeting

behavior through enhanced permeability and retention (EPR) effect [53–55]. In order to increase the aggregation in specific areas, such as tumors, dendrimers are able to be conjugated with specific targeting ligands to improve their specificity and cellular uptake [56, 57]. Besides, the attached surface groups affect the solubility and biocompatibility of dendrimers [15, 58]. Through appropriate surface modification, dendrimers are able to have high water solubility and improved biocompatibility. These characteristics may impart the dendrimer-based contrast agents a better application prospect in clinical practice than conventional small molecular contrast agents.

4.2 Preparation of Dendrimer-Based Nanoplatforms

Dendrimer-based contrast agents can be prepared in a variety of ways. For instance, dendrimers are able to connect with iodinated small molecular CT contrast agents, fluorescent molecules, gadolinium (Gd) or radionuclide chelators for CT [59–61], fluorescence [62–64], MR [65–67], and radionuclide-based imaging [68–72]. In addition, dendrimers can be utilized as either templates or stabilizer to construct gold (Au) or iron oxide NPs for CT [52] or MR imaging [73, 74], and functionalized dendrimers can also be assembled onto preformed iron oxide NPs for MR imaging [25, 75]. Furthermore, the versatile dendrimer nanotechnology allows for the incorporation of different types of contrast agents for dual or multimodality imaging. For instance, Au NPs can be formed using dendrimers as templates, and then Gd, radionuclide chelator complexes, or fluorescent molecules can be further modified on the surface of dendrimers for CT/MR [76, 77], SPECT/CT [69], or CT/MR/optical imaging applications [34]. The facile modification of dendrimer surface with different substances and convenient strategies used to generate multifunctional nanoparticles render the dendrimers with great advantages and capacities for different imaging applications.

5 Key Research Findings

5.1 SPECT Imaging

SPECT is a nuclear medicine imaging technique using single photon radionuclides which emit gamma (γ) rays in the energy range of approximately 75 to 360 keV [78, 79]. SPECT imaging with extremely high sensitivity is applicable to tomographic and quantitative functional information in a living subject [35]. For SPECT imaging, small amounts of compounds were labeled by radionuclides called radiotracers which can be applied as noninvasive diagnostic agents. Following administration of radiotracers to a patient, the γ-rays from radionuclides can be directly measured by SPECT detectors. Generally, radionuclides used in SPECT imaging include technetium-99 m (^{99m}Tc), indium-111 (^{111}In), iodine-123 (^{123}I), and galium-67 (^{67}Ga) with half-lives varying from several hours to a few days [80]. Among those, ^{99m}Tc is so far the most used radionuclide in SPECT imaging [81–83]. This is due to its latent chemical properties for labeling and highly attractive physical properties such as

appropriate half-life (6.02 h) and low-energy γ-ray (140 keV), which is favorable for both effective imaging and radiation safety. Furthermore, ^{99m}Tc can be conveniently obtained from a ^{99}Mo/^{99m}Tc generator with low production cost [82].

Over the last several decades, diethylenetriaminepentaacetic acid (DPTA) chelator [84–86], an aminopolycarboxylic acid consisting of a diethylenetriamine backbone with five carboxymethyl groups, has played a significant role in the field of SPECT imaging applications [87–89]. The dendrimer scaffolds conjugated with DTPA can be readily labeled with various radionuclides, such as ^{99m}Tc and ^{111}In. For instance, Zhang et al. reported the synthesis and SPECT imaging of ^{99m}Tc-labeled dendrimer-based nanoparticles using generation 5 (G5) polyamidoamine (PAMAM) dendrimers as a template [90]. In this study, dendrimers were first partially acetylated (Ac) to improve solubility and reduce nonspecific cellular uptake. Then folic acid (FA) was linked on the surface of PAMAM dendrimers as a targeting molecule to FA receptor (FAR)-overexpressing cancer cells, and multiple DTPA chelators were conjugated for ^{99m}Tc labeling. The formed ^{99m}Tc-G5-Ac-FA-DTPA conjugate had a radiochemical yield up to 98.9%, excellent stability, and rapid blood clearance. Preferential uptake in the FAR-positive tumors was confirmed by biodistribution and micro-SPECT imaging studies in KB tumor-bearing nude mice. In the following work, the same authors investigated the effects on the uptake of ^{99m}Tc-labeled dendrimers in tumors using different FA linking strategies [91]. PEGylated FA and FA were respectively modified onto the surface of acetylated G5 PAMAM dendrimers, followed by linking DTPA chelators for the labeling of ^{99m}Tc to form ^{99m}Tc-G5-Ac-pegFA-DTPA and ^{99m}Tc-G5-Ac-FA-DTPA. Both of the biodistribution and micro-SPECT imaging studies showed that PEGylated FA dendrimer conjugate had higher specific accumulation in tumor than that of ^{99m}Tc-G5-Ac-FA-DTPA, while no obvious uptake of radiolabeled dendrimer without folic acid was observed in tumor (Fig. 12.1). These results demonstrated that indirect FA conjugation through PEG spacer was able to enhance the accumulation in tumors more significantly than direct FA conjugation via EDC chemistry. Subsequently, they attempted to employ avidin instead of folic acid on dendrimer surface to decrease the accumulation of ^{99m}Tc-labeled conjugate in the kidneys [92]. It seemed that this method was able to gain a low uptake in the kidney but very high accumulation in the liver and spleen.

Beyond the use of ^{99m}Tc, ^{111}In is another promising radionuclide for SPECT imaging, which is produced in a cyclotron from the proton irradiation reaction of cadmium [93]. ^{111}In with a decay mode of electron capture emits 173 and 247 keV γ-rays and has a relatively long half-life (2.8 days) [94–96]. Like ^{99m}Tc, ^{111}In can be effectively chelated by DTPA ligands [97]. Kojima et al. synthesized ^{111}In-labeled DTPA-conjugated polymers using G4 acetylated PAMAM dendrimer (Ac-den) and collagen peptide-conjugated dendrimer (CP-den) (Fig. 12.2a, b) and investigated their behaviors in vivo by micro-SPECT imaging following subcutaneous injection into tumor-bearing mice, respectively (Fig. 12.2c) [98]. These ^{111}In-DTPA-bearing dendrimers were largely retained at the injection site for at least 1 day. Notably, because of higher molecular weight, the retention time of CP-den-DTPA was longer than that of Ac-den-DTPA. Thus, thanks to the prolonged retention around the subcutaneous injection site, these polymers with controlled-release drug delivery systems might be beneficial for long-term treatment.

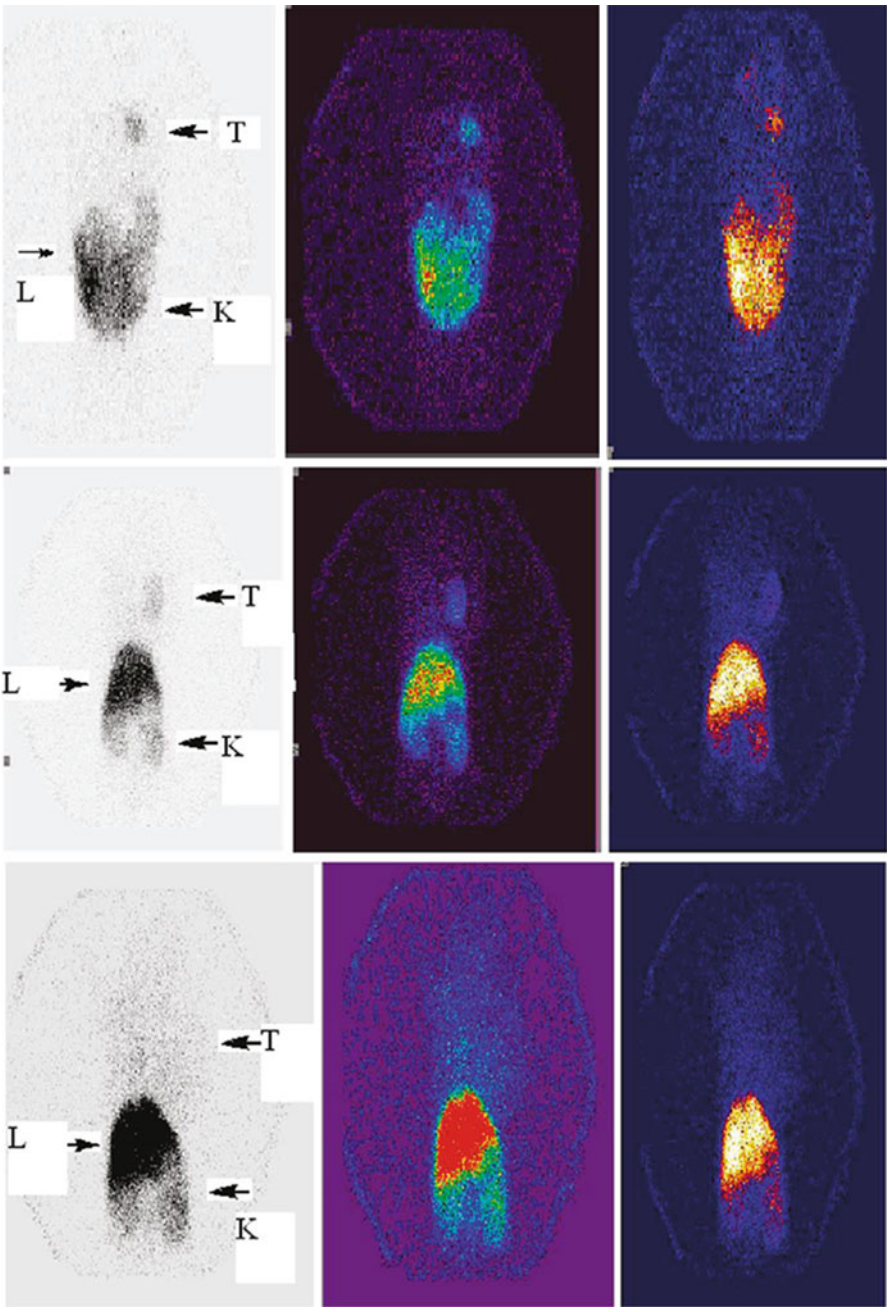

Fig. 12.1 Micro-SPECT images of KB-bearing nude mice at 4 h: *T*, tumor; *L*, lungs; *K*, kidney ((upper) ^{99m}Tc-G5-Ac-pegFA-DTPA, (middle) ^{99m}Tc-G5-Ac-FA-DTPA, (lower) ^{99m}Tc-G5-Ac-DTPA)) (Reprinted (adapted) with permission from Ref. [91]. Copyright (2010) American Chemical Society)

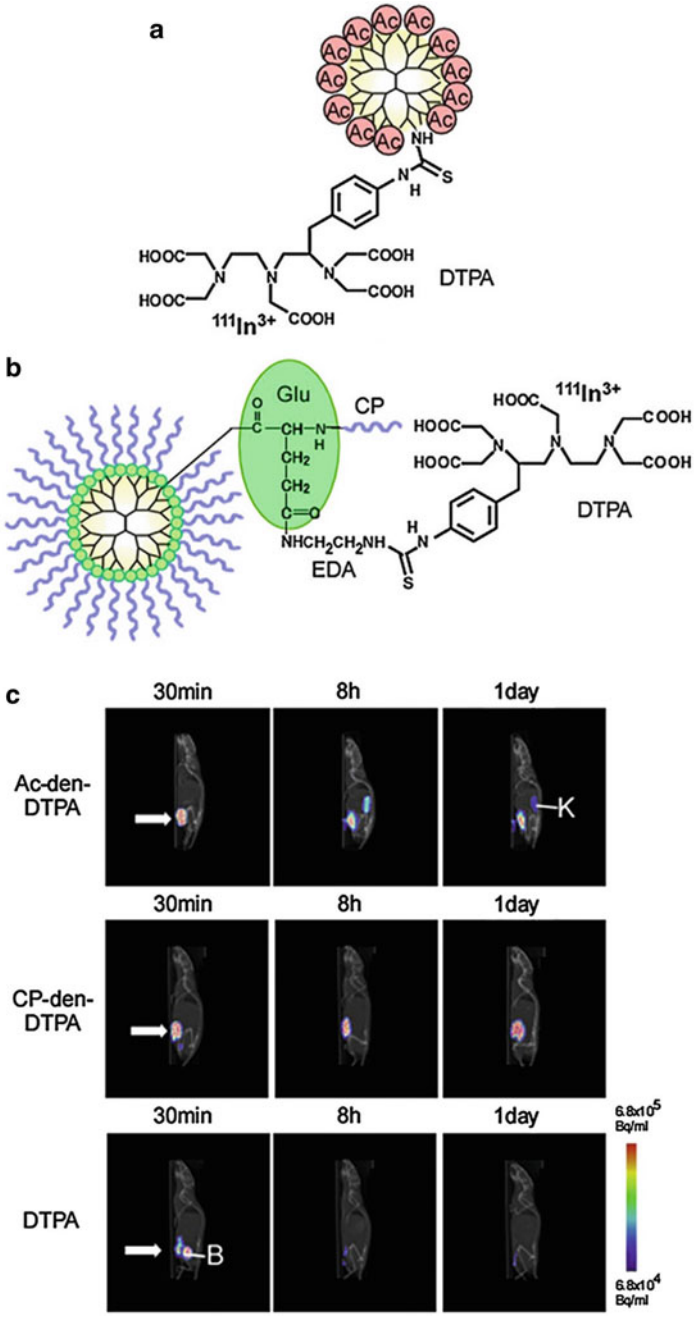

Fig. 12.2 (**a**) ^{111}In-labeded acetylated (Ac) dendrimer with DTPA (Ac-den–DTPA), (**b**) ^{111}In-labeded collagen peptide-conjugated (CP) dendrimer with DTPA (CP-den–DTPA), (**c**) SPECT/CT imaging of mice subcutaneously injected with Ac-den-DTPA, CP-den-DTPA, and unconjugated

The lymphatic system, especially the sentinel lymph node (SLN), plays a vital role in the metastatic spread of various cancer cells [99–101]. Within the fields of cancer therapy and diagnosis, a great deal of attention has been attracted in the noninvasive imaging of SNL using dendrimer-based nanoparticles [102, 103]. For example, Sano et al. prepared ^{111}In-labeled G4 PAMAM dendrimers conjugated with DTPA, polyethyleneimine (PEI), and γ-polyglutamic acid (γ-PGA) and evaluated their feasibilities as nanoprobes for SPECT imaging of SLN [104]. It seemed that the synthesized ^{111}In-DTPA-G4/PEI/γ-PGA with high biocompatibility could be highly taken up by macrophage cells in vitro comparable to the ^{111}In-DTPA-G4/PEI without γ-PGA modification, which might be due to the mechanisms of phagocytosis and γ-PGA-specific pathway. Intradermal administration of ^{111}In-labeled dendrimer conjugates into rat footpads, when compared with ^{111}In-DTPA-G4/PEI and ^{111}In-DTPA-G4/PEI/γ-PGA, the latter had a relative fast clearance from the injection site, significantly higher radioactive uptake in the first draining popliteal LN, and low radioactivity in the other tissues including the liver, spleen, and kidneys, which was confirmed by micro-SPECT imaging studies (Fig. 12.3). Subsequently, Niki et al. systematically evaluated 12 types of different generations (G2, G4, G6, and G8) of dendrimers with different terminal groups (amino, carboxyl, and acetyl) to determine the optimal one for sentinel lymph node imaging [105]. The SPECT imaging studies showed that high-generation (greater than G4) PAMAM dendrimers with carboxyl-termini were able to significantly accumulate at the SLN, which might have important effects on the development of dendrimer-based SLN imaging agents and SLN-targeted drug carriers.

5.2 SPECT/CT Imaging

CT is known as one of the most useful imaging techniques in modern research and clinical settings, which can be applied in the detection of tissues, organs, and blood vessels [106–108]. CT contrast agents are regularly introduced in order to improve contrast and acquire desirable imaging quality. Commercially available CT contrast agents are usually iodinated small molecules with the drawbacks of rapid clearance from blood after injection, latent renal toxicity at a relatively high concentration, and nonspecificity to tissues and organs, which restricts the scope of applications [45].

Recently, there is great interest in the development of dendrimer-based nanoparticles for CT imaging to overcome these drawbacks caused by the small molecular iodinated contrast agents [109–111]. Due to unique structural features of

Fig. 12.2 (continued) DTPA at different times after injection. Arrows indicate the injection site, and L, K, and B indicate the liver, kidney, and bladder, respectively (Reprinted (adapted) with permission from Ref. [98]. Copyright (2014) Elsevier)

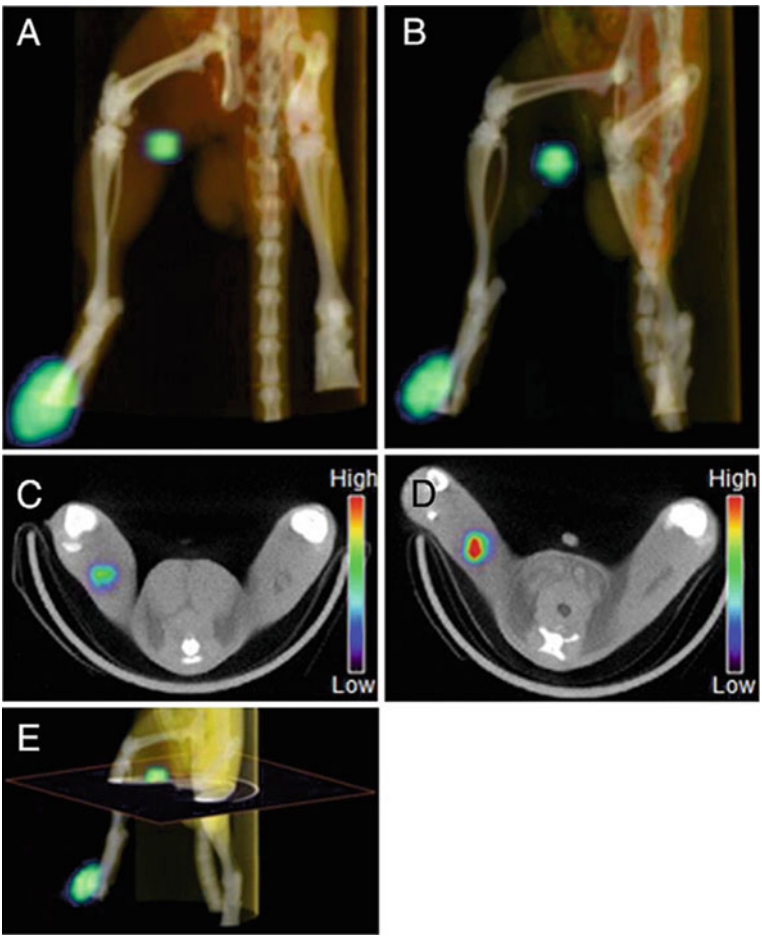

Fig. 12.3 SPECT/CT images (**a**–**e**) after the injection of ^{111}In-DTPA-G4/PEI (**a**, **c**) or ^{111}In-DTPA-G4/PEI/γ-PGA (**b**, **d**) into footpads of SD rats (DTPA-G4: 10 μg/mL, 1.0–1.7 MBq/200 μL in 5% glucose/rat). Panels (**c**) and (**d**) are 2D transaxial images including lymph nodes constructed from 3D images (**a** and **b**) as shown in (**e**). ^{111}In-DTPA-G4/PEI/γ-PGA (**b**, **d**) clearly visualized the popliteal lymph nodes (sentinel LNs in this model) compared to ^{111}In-DTPA-G4/PEI (**a**, **c**) (Reprinted (adapted) with permission from Ref. [104]. Copyright (2014) Elsevier)

dendrimers, the developed dendrimer-based CT contrast agents can also be labeled with ^{99m}Tc for SPECT/CT imaging to afford diagnosis accuracy. For instance, Criscione et al. conjugated triiodinated moieties and ^{99m}Tc on the surface of G4 PAMAM dendrimers modified with *m*PEG (Fig. 12.4) [112]. The iodinated dendritic NPs with a diameter of 12.4 nm displayed similar X-ray attenuation properties to the small molecule iodinated contrast agents (Omnipaque 350) routinely used in clinical

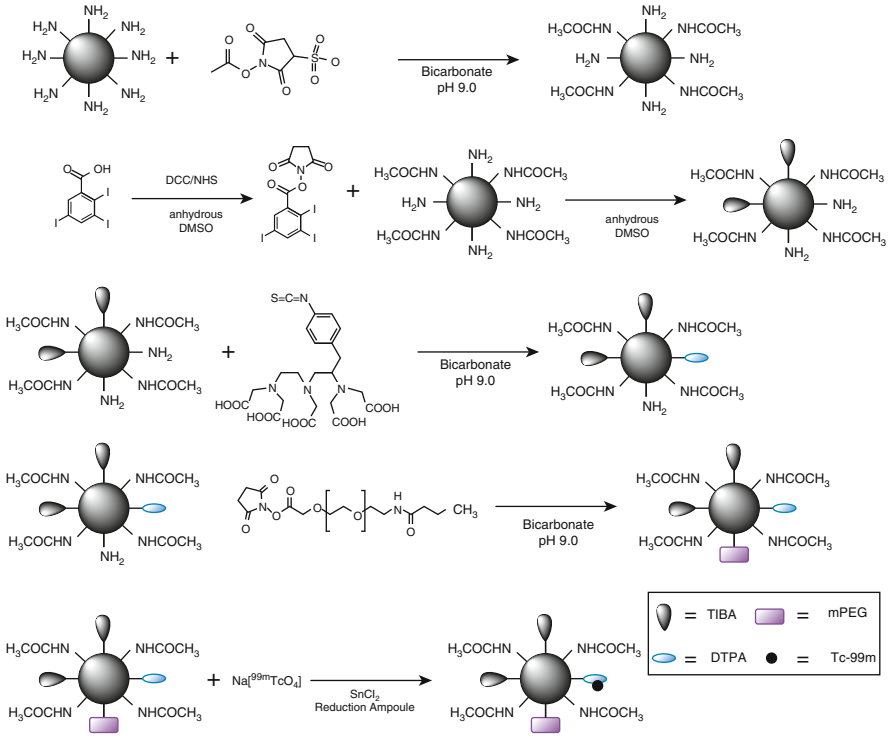

Fig. 12.4 Schematic of the synthesis of ^{99m}Tc-labeled G4-[[[[Ac]-TIBA]-DTPA]-mPEG12] (Reprinted (adapted) with permission from Ref. [112]. Copyright (2011) American Chemical Society)

applications and possessed long enough intravascular residence time, favorable contrast-to-noise ratio for serial intravascular, and blood pool imaging with both SPECT and CT. However, further evaluations of this potential SPECT/CT agent including toxicity in vitro and in vivo have not been investigated in the literature.

Meanwhile, Au NPs have received great attention as CT contrast agents due to their higher atomic number than that of iodine for iodine-based small molecular contrast agents, stronger X-ray attenuation coefficient, and better biocompatibility than iodine-based CT contrast agents [13, 113–115]. In a recent study, Shi and coworkers reported ^{99m}Tc-labeled multifunctional dendrimer-entrapped gold nanoparticles (Au DENPs) for tumor-targeted SPECT/CT imaging using amine-terminated G2 PAMAM dendrimers as templates [69]. The low-generation dendrimers were functionalized with DTPA via an amide linkage and targeting ligand FA via a PEG spacer and then used to entrap Au core NPs (Fig. 12.5). The developed Au DENPs with an average Au core diameter of 1.6 nm had excellent solubility in water, satisfactory stability, and biocompatibility in a given concentration range. Biodistribution and SPECT/CT imaging studies further demonstrated that

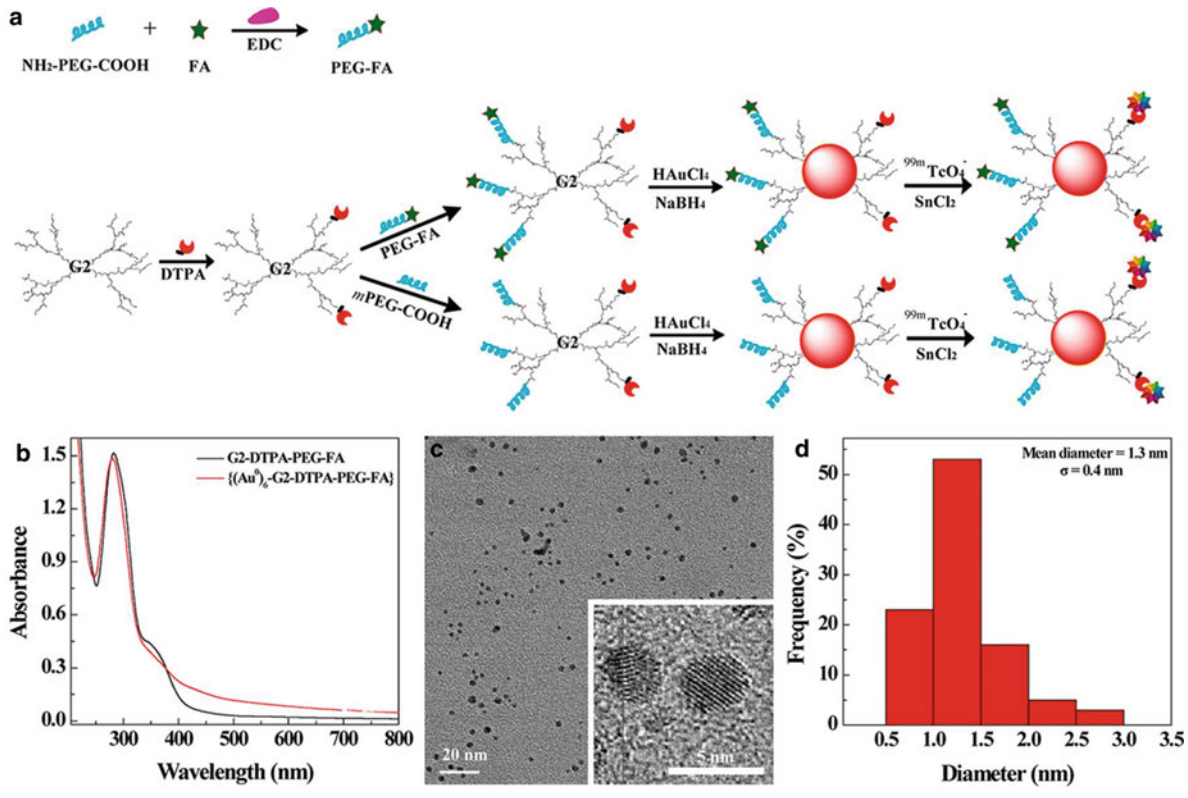

Fig. 12.5 (**a**) Schematic illustration of the synthesis of FA-PEG-COOH segment, $(Au_0)_6$-G2-DTPA(^{99m}Tc)-PEG-FA ENPs, and $(Au_0)_6$-G2-DTPA(^{99m}Tc)-mPEG DENPs. (**b**) UV-vis spectra of G2-DTPA-PEG-FA and $(Au_0)_6$-G2-DTPA-PEG-FA DENPs. (**c**) TEM image and (**d**) size distribution histogram of the

the formed multifunctional Au DENPs had a great potential to be utilized as an effective and economic nanoplatform for dual-mode imaging of FAR-overexpressing tumors (Fig. 12.6).

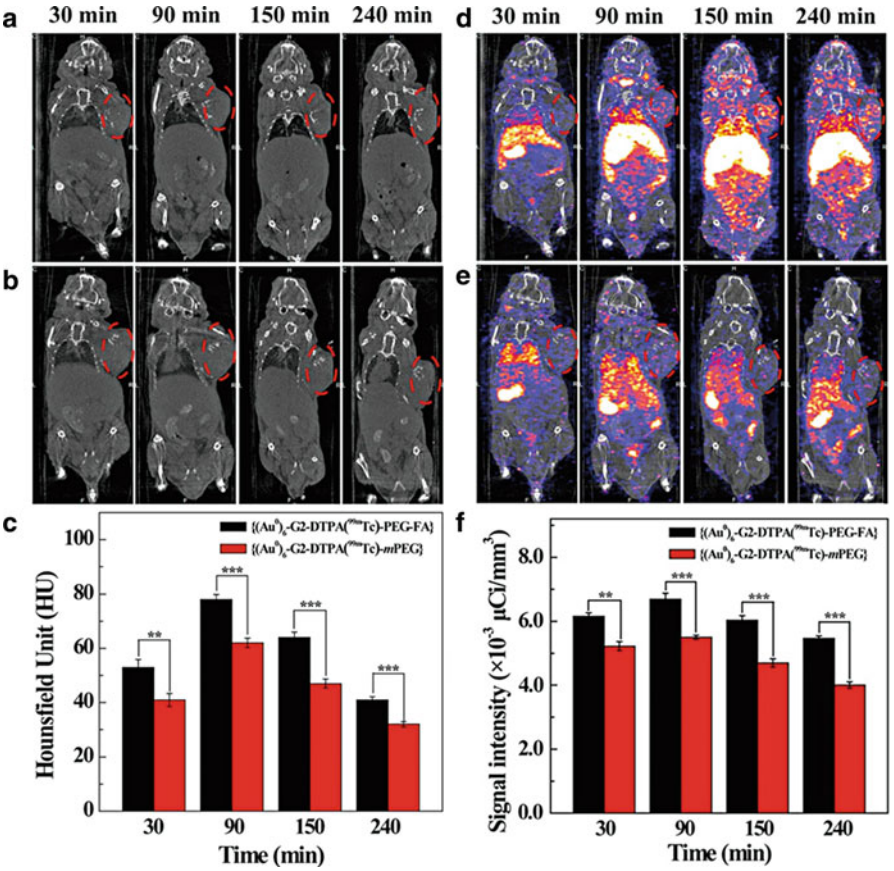

Fig. 12.6 In vivo CT images (**a** and **b**) and signal intensity (**c**) of tumors after intravenous injection of the $\{(Au^0)_6$-G2-DTPA(^{99m}Tc)-PEG-FA$\}$ (**a**) or $\{(Au^0)_6$-G2-DTPA(^{99m}Tc)-mPEG$\}$ (**b**) DENPs ([^{99m}Tc] = 740 MBq·mL^{-1}, [Au] = 0.08 M, in 100 μL PBS) at different time points postinjection. In vivo SPECT/CT images of tumors (**d** and **e**) and SPECT signal intensity of tumors (**f**) after intravenous injection of the $\{(Au^0)_6$-G2-DTPA(^{99m}Tc)-PEG-FA$\}$ DENPs (**d**) or $\{(Au^0)_6$-G2-DTPA (^{99m}Tc)-mPEG$\}$ DENPs (**e**) ([^{99m}Tc] = 740 Bq·mL^{-1}, [Au] = 0.08 M, in 100 μL PBS) at different time points postinjection. The dashed red circles indicate the tumor sites (Reprinted (adapted) with permission from Ref. [69]. Copyright (2016) American Chemical Society)

Fig. 12.5 (continued) $(Au_0)_6$-G2-DTPA-PEG-FA DENPs. Inset in panel c shows the high-resolution TEM image of the Au core particles (Reprinted (adapted) with permission from Ref. [69]. Copyright (2016) American Chemical Society)

5.3 SPECT/MR Imaging

MR imaging has been evolved as an indispensable imaging technique for clinical diagnosis due to its admirable spatial resolution, noninvasive nature, and no ionizing radiation [116, 117]. Similarly to CT imaging, contrast agents are commonly required in clinical MR applications to improve the visibility of internal tissue or organ structures. The most generally used compounds for contrast enhancement are Gd (III)-based small molecules, which also suffer from some disadvantages including rapid excretion [55], relatively low contrast effect [118], possible renal damage [119], and lack of sufficient sensitivity and specificity [120]. Taking advantage of the superiorities of dendrimers discussed above, a lot of dendrimer-based MR contrast agents have been prepared to eliminate the defects of Gd-based contrast agents [65, 121, 122]. In most cases of T_1-weighted MR imaging, dendrimers serve as scaffolds to load multiple copies of small molecular Gd(III) complexes, typically Gd(III) chelated with tetraazacyclododecane tetraacetic acid (DOTA) [65] or DPTA [121, 122]. Then these dendrimers containing Gd(III) can be further labeled with radionuclides for dual-mode SPECT/MR imaging. Interestingly, except nonradioactive ^{157}Gd used as MRI contrast agent, ^{147}Gd ($E_\gamma = 229$ keV, $t_{1/2} = 38.1$ h) is γ-ray-emitting radionuclides which may be exploited for SPECT imaging [123]. Recently, Rahmania et al. reported radiogadolinium(III) DOTA-based PAMAM G3 dendrimers linked with monoclonal antibody trastuzumab as a SPECT/MR imaging agent for diagnosis of HER-2-positive breast cancer [123]. It seemed that the radiogadolinium-labeled dendrimers had good radiochemical purity and stability. However, more detailed investigation of this SPECT/MR agent including toxicity and performance in vitro and in vivo has not been performed in this study. In a recent study, Luo et al. developed a facile approach to prepare a manganese (Mn) and ^{99m}Tc-coloaded dendrimeric nanoprobe for tumor-targeted SPECT/MR imaging applications [68]. G5 PAMAM dendrimers were used as a platform to link FA and DOTA, followed by complexation with Mn(II) for T_1-weighted MR imaging and simultaneously labeling with ^{99m}Tc for SPECT imaging both via DOTA chelation. The formed multifunctional dendrimer-FA conjugates before ^{99m}Tc labeling had good water solubility, cytocompatibility, and stability and were able to rapidly accumulate and reach the peak value in the tumor region within 2 h for MR imaging (Fig. 12.7), which was also confirmed by SPECT imaging (Fig. 12.8). These results revealed that this nanoprobe could be used for specific SPECT/MR imaging of cancer cells in vivo.

5.4 SPECT/Optical Imaging

Fluorescence imaging provides unique advantages in terms of high sensitivity, multiplex detection capabilities, and inexpensiveness. Nevertheless, it primarily depends on suitable markers such as fluorescent dyes or proteins, with good stability, excellent biocompatibility, and high specificity and sensitivity to ensure the images with splendid temporal and spatial resolution [48]. With the quite rigid molecular structure, dendrimers have the blue fluorescence emission property

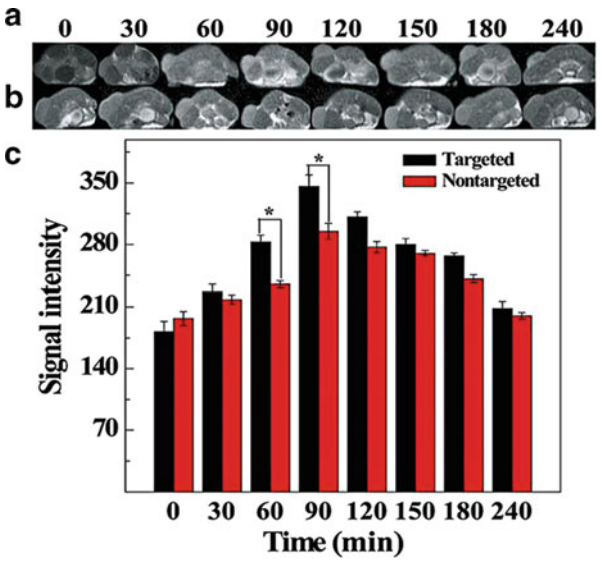

Fig. 12.7 In vivo T_1-weighted MR images (**a** and **b**) and signal intensity (**c**) of tumors after intravenous injection of the nontargeted G5.NHAc-FI-DOTA(Mn) (**a**) or targeted G5.NHAc-FI-DOTA(Mn)-FA (**b**) dendrimers (300 mg Mn, in 0.3 mL PBS) at different time points postinjection (Ref. [68] – Reproduced by permission of The Royal Society of Chemistry)

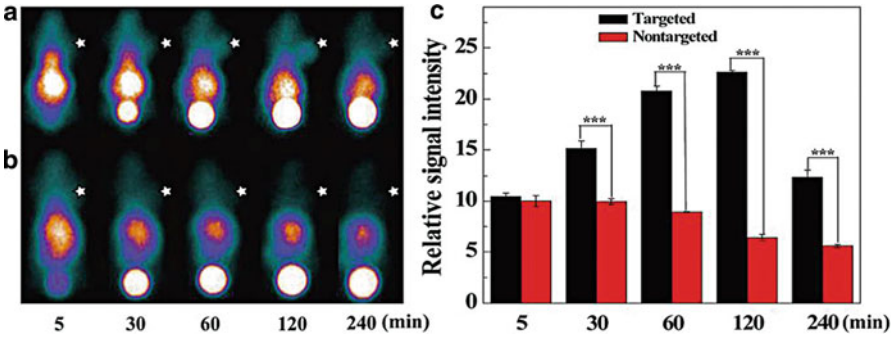

Fig. 12.8 In vivo SPECT images (**a** and **b**) and SPECT signal intensity (**c**) of tumors after intravenous injection of the targeted G5.NHAc-FI-DOTA(Mn/^{99m}Tc)-FA (**a**) and nontargeted G5.NHAc-FI-DOTA(Mn/^{99m}Tc) (**b**) dendrimers (3 mCi ^{99m}Tc, in 0.2 mL PBS) at different time points postinjection (Ref. [68] – Reproduced by permission of The Royal Society of Chemistry)

[124, 125]; however, the intrinsic fluorescence quantum yield is quite low and unsuitable for clinical applications. Therefore, dendrimer-based nanomaterials have been broadly investigated as fluorescence imaging agents in order to enhance the fluorescence quantum yield [124]. In general, fluorescent molecules can be readily modified onto the surface or be loaded within the interior of dendrimers as fluorescence probes. To achieve different imaging purposes, these probes can be subsequently labeled with ^{99m}Tc for dual-mode SPECT/fluorescence imaging. For instance, Tsuchimochi et al. developed PAMAM G3 dendrimer-coated silica nanoparticles loaded with ^{99m}Tc and indocyanine green

(ICG) for SPECT/NIR imaging of SNL [126]. The formed PAMAM-coated silica nanoparticles with a diameter of 30–50 nm were injected into the tongue of rats. In the animal studies, these nanoparticles were able to clearly depict sentinel lymph nodes in real time with the use of dual-mode imaging.

5.5 Theranostics

The rapid development of imaging techniques and drug delivery systems has offered opportunities in a relatively new area called "theranostics" [127, 128]. For theranostics, it is essential to combine diagnostic and therapeutic functionalities into a single system, to develop more precise and personalized therapies for various diseases. A convenient way in constructing theranostic agents is to load therapeutic functions on existing imaging nanoprobes. Besides various imaging applications, dendrimer-based nanomaterials have been known with this capability and used as carriers for drug, gene, and therapeutic radionuclide delivery [46, 128]. Among massive therapeutic radionuclides, ^{131}I is one of the most common therapeutic radionuclides in the clinic, because of its relative long half-life (8.01 days) and appropriate beta radiation energy (606 keV) for radiotherapy [70, 129, 130]. Moreover, ^{131}I emits a γ-ray (364 keV) for SPECT imaging which renders its feasibility for theranostic applications. While another important radioisotope of iodine, ^{125}I with less energy γ-ray (35.5 keV) is poorly suited for imaging but convenient for radioimmunoassay test, implantation therapy, and method development due to its long half-life (60.1 days) [131, 132].

Merkel et al. reported a family of triazine dendrimers as nonviral gene delivery systems with high transfection efficacy [133, 134]. Then these flexible triazine dendrimer-based siRNA complexes were synthesized for gene delivery systems and labeled with ^{111}In via DTPA for SPECT imaging to identify efficient siRNA delivery in vivo [135]. Interestingly, simulated thermodynamic approach was employed to explain the interactions of dendrimers with siRNA and compared with the experimental data including siRNA complexation, complex stability, size, and zeta potentials. In their following work, Lee et al. designed and developed a G3 triazine dendrimer with 8 PEG chains and 16 paclitaxel groups (Fig. 12.9) [136]. Molecular dynamic simulations revealed that the water penetration and accessibility of novel complexes were better than their previous constructs, but the computed dimension of complexes was significantly smaller than the 15.8 nm obtained from experiment. Slow and identical release of paclitaxel was observed in plasma in drug release studies. Biodistribution and SPECT/CT imaging of ^{125}I–labeled complexes suggested significant persistence in the vasculature with slow clearance and high tumor uptake while low levels of radiolabeled dendrimer in the lung, liver, and spleen (Fig. 12.10). In another study, Xiao et al. reported a multifunctional telodendrimer-based micelle system for SPECT imaging and delivery of chemotherapy agents [137]. The telodendrimer was covalently modified with ^{125}I for SPECT/CT imaging and loaded with ^{14}C–paclitaxel for pharmacokinetics and biodistribution studies, respectively. SPECT/CT imaging showed that ^{125}I–labeling nanomicelles were preferential uptaken

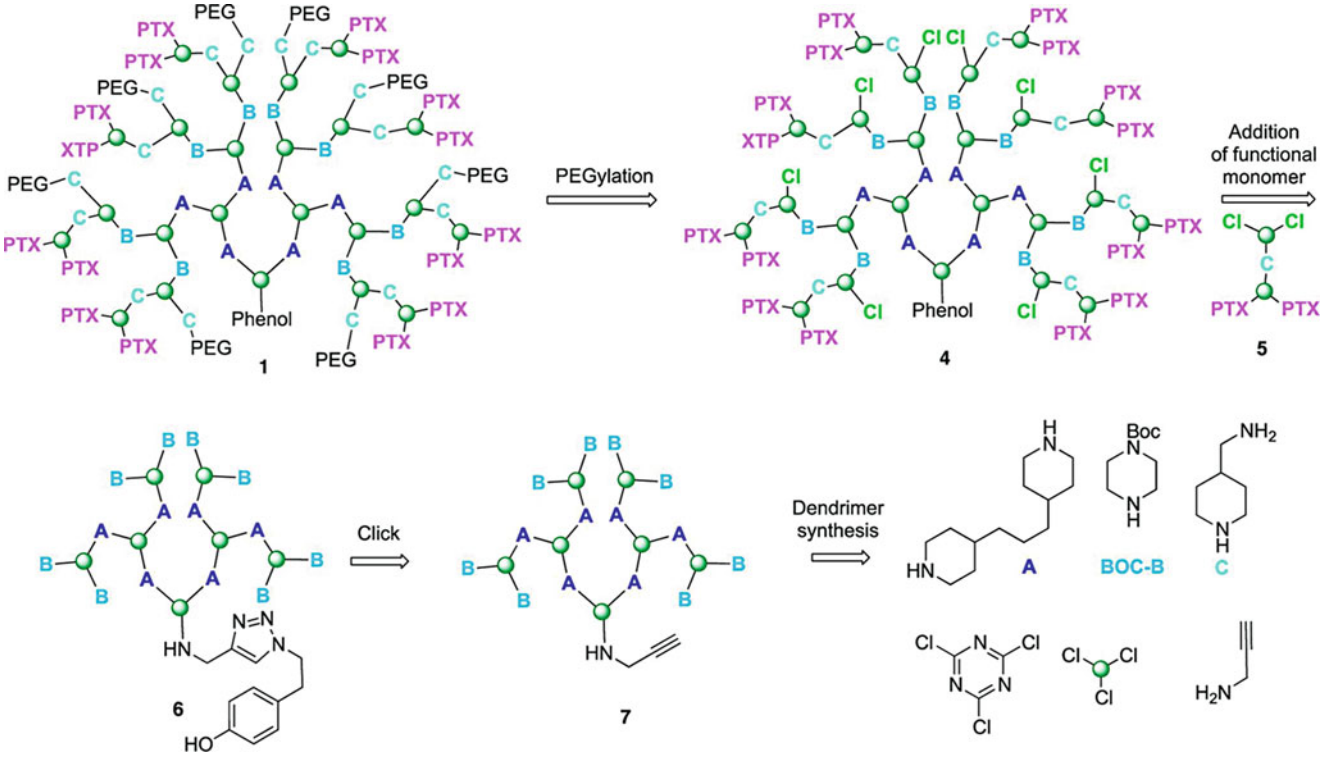

Fig. 12.9 Target 1 derives from a two-step PEGylation procedure of 4. Intermediate 4 results from reaction of the functionalized dichlorotriazine bearing two paclitaxel groups (PTX), 5, with dendrimer 6. Dendrimer 6 comes from click reaction of 7, which derives from some of the building blocks identified (Reprinted (adapted) with permission from Ref. [136]. Copyright (2013) American Chemical Society)

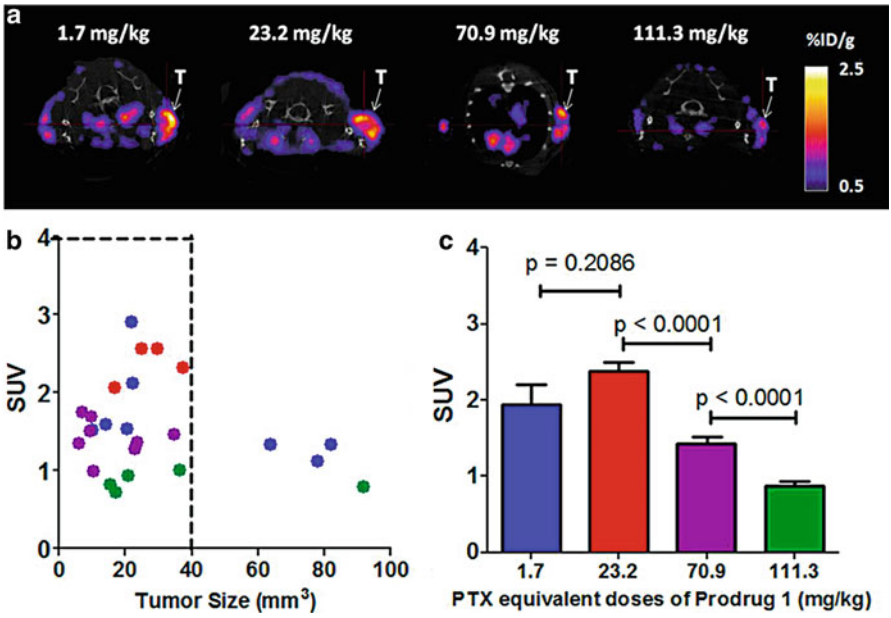

Fig. 12.10 Tumor saturation dose evaluation of ^{125}I-1 in PC-3 tumor-bearing mice: 1.7 mg/kg (blue), 23.2 mg/kg (red), 70.9 mg/kg (purple), and 111.3 mg/kg (green). (**a**) Representative transaxial SPECT/CT images of PC3 tumor in SCID mice (48 h p.i.). Tumors are indicated by white arrows. (**b**) Tumor uptake of ^{125}I-1 versus tumor size. Tumors smaller than 100 mm^3 were selected for the evaluation. (Number of tumors evaluated in each group: 7 (1.7 mg/kg); 5 (23.2 mg/kg); 8 (70.9 mg/kg); 5 (111.3 mg/kg)). (**c**) Tumor uptake levels of the four dosing groups in tumors smaller than 40 mm^3. (Number of tumors evaluated in each group: 4 (1.7 mg/kg); 5 (23.2 mg/kg); 8 (70.9 mg/kg); 4 (111.3 mg/kg)). SUV is standardized uptake value of the labeled prodrug (Reprinted (adapted) with permission from Ref. [136]. Copyright (2013) American Chemical Society)

by tumor tissues with slow clearance, and the biodistribution data of ^{14}C–paclitaxel-loaded nanomicelles also confirmed the increased accumulation at the tumor site with slower pharmacokinetics than Taxol. The results suggested that nanomicelle-loaded paclitaxel might be used as a promising nanocarrier for imaging-guided drug delivery.

In a recent study, Shi group and the coworkers reported a series of multifunctional dendrimers labeled with ^{131}I for targeted SPECT imaging and radiotherapy of different cancers [70, 129, 130]. In these studies, G5 amine-terminated PAMAM dendrimers were used as platforms to be sequentially conjugated with PEG, targeting agent biotoxins or FA, and 3-(4-hydroxyphenyl)propionic acid-OSu (HPAO). These were followed by acetylation of the remaining dendrimer terminal amines and radiolabeling with ^{131}I directly through HPAO to form the targeted theranostic dendrimeric nanoplatforms (Fig. 12.11). The formed ^{131}I–labeled multifunctional dendrimers with good cytocompatibility and organ compatibility could be used as promising nanoplatforms for SPECT imaging and radiotherapy of different types of MMP2 or FAR-overexpressing cancers (Fig. 12.12).

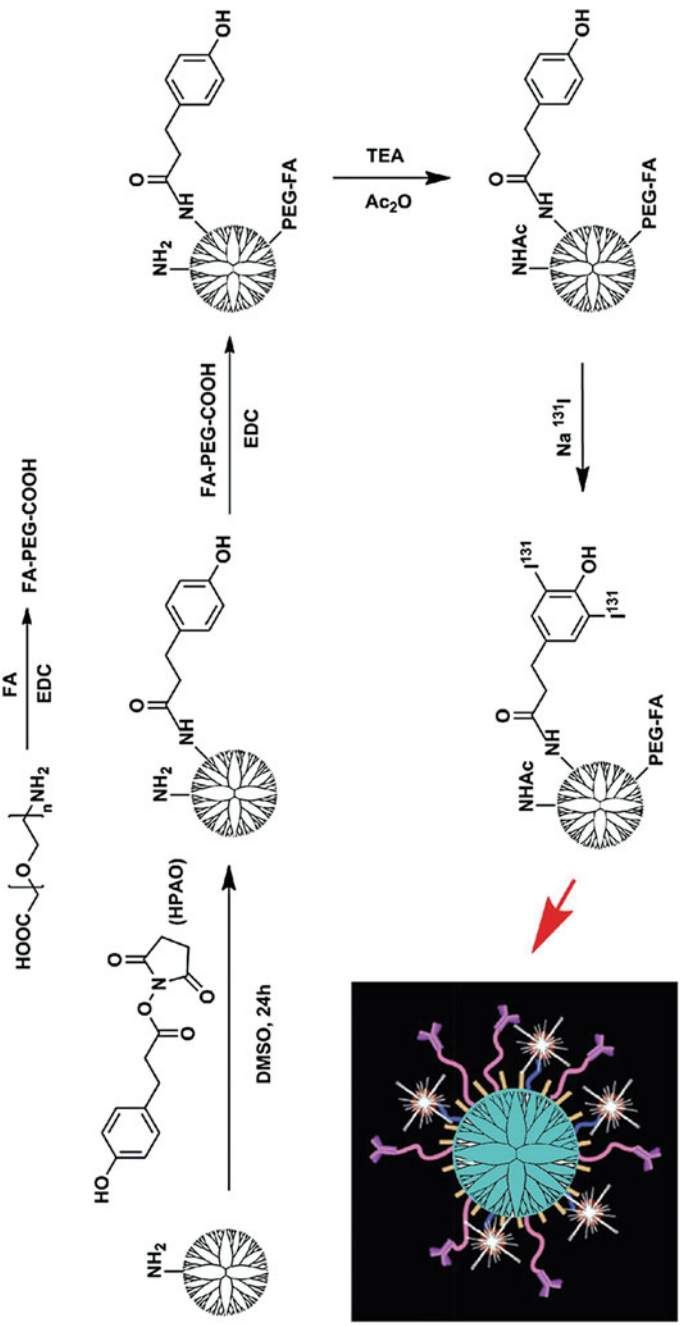

Fig. 12.11 Schematic illustration of the synthesis of the ^{131}I–G5·NHAc-HPAO-PEG-FA dendrimers (Ref. [129] – Reproduced by permission of The Royal Society of Chemistry)

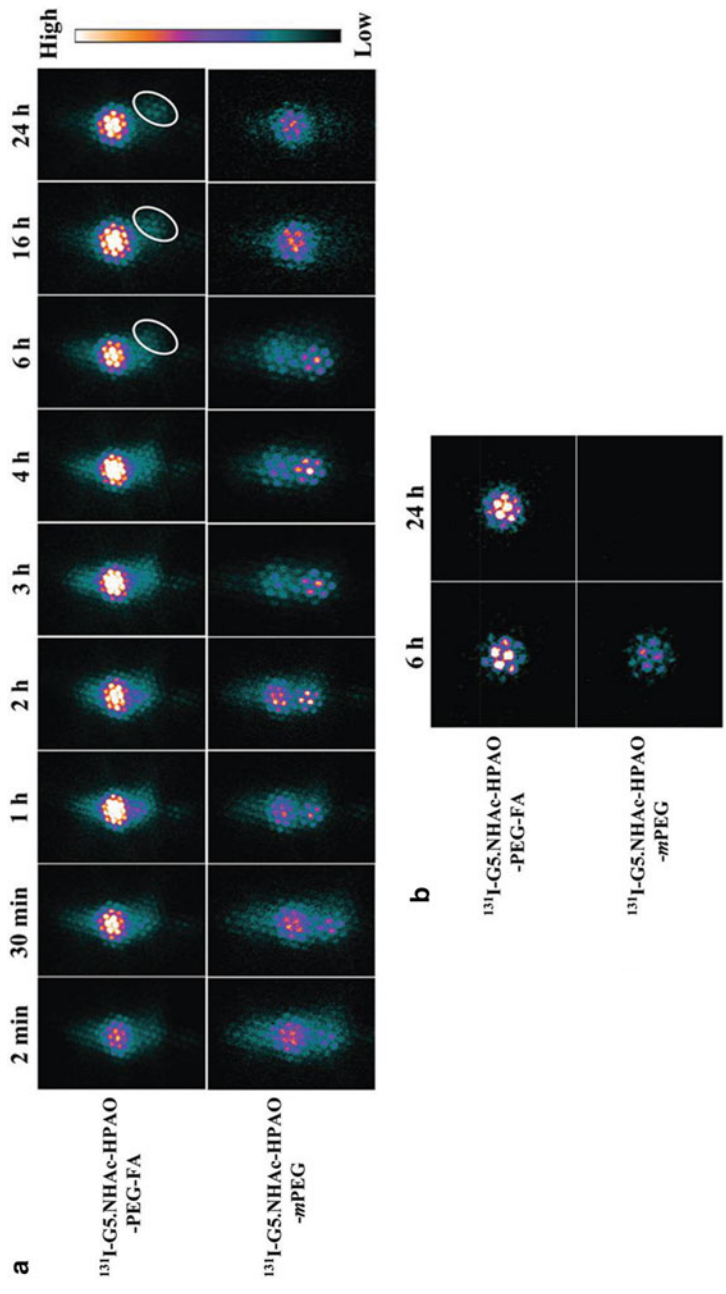

Fig. 12.12 SPECT images of the nude mice bearing C6 xenografted tumors at different time points post-intravenous injection of the ^{131}I–G5·NHAc-HPAO-PEG-FA and ^{131}I–G5·NHAc-HPAO-mPEG dendrimers (tumor site was marked by white circle) (**a**) and SPECT images of ex vivo tumors (**b**) (Ref. [129] – Reproduced by permission of The Royal Society of Chemistry)

6 Conclusion and Future Perspectives

In summary, we have reviewed the use of dendrimer-based nanoplatforms for SPECT imaging applications including single-mode SPECT imaging, dual-mode SPECT/CT, SPECT/MR, and SPECT/optical imaging and theranostic applications. In view of the unique structural features of dendrimers, abundant dendrimer-based nanomaterials as platforms can be formed since they can be functionalized with fluorescent dyes, iodinated CT contrast agents, Gd, and radionuclides on the periphery and can be used to entrap, stabilize, or assemble Au and metal oxide nanoparticles, generating all sorts of imaging agents. The functionalized dendrimers have been used for imaging of blood pool, lymph nodes, major organs, cancer, and other biological systems. Importantly, these developed dendrimer-based imaging agents can be further modified with targeting ligands to improve specificity and selectivity and loaded drugs, genes, or therapeutic radionuclides for theranostic applications, which is of great importance for precise cancer diagnosis and imaging-guided drug delivery applications.

In spite of comprehensive investigation on dendrimer-based nanoplatforms, this growing area of research still remains largely underground, and a great number of challenges are needed to be explored [48, 127]. For instance, the toxicity of dendrimer-based contrast agents is one of inevitable issues, particularly the large molecule systems with slow clearance and latent renal damage from Gd-containing dendrimeric nanoparticles. In addition, more types of dendrimer-based nanoplatforms should be developed in order to satisfy different requirements. For instance, to expand the scope of imaging, radionuclides can be modified on the surface of dendrimer-based iron oxide NPs for SPECT and T_2-weighted MR imaging. Furthermore, with the ability to equip therapeutic modules in dendrimer platforms via many different approaches, it is requisite to develop various multifunctional dendrimers by integrating drugs, genes, or therapeutic radionuclides into dendrimer-based imaging agents for theranostic applications.

Acknowledgments This research is financially supported by the National Natural Science Foundation of China (81671712, 81401440), the Program for Professor of Special Appointment (Eastern Scholar) at Shanghai Institutions of Higher Learning, and the Sino-German Center for Research Promotion (GZ899). L. Zhao thanks the support from the Shanghai Sailing Program (16YF1409300).

References

1. Collins FS, Varmus H (2015) A new initiative on precision medicine. N Engl J Med 372 (9):793–795
2. Jameson JL, Longo DL (2015) Precision medicine – personalized, problematic, and promising. N Engl J Med 372(23):2229–2234
3. Weissleder R, Pittet MJ (2008) Imaging in the era of molecular oncology. Nature 452 (7187):580–589
4. Pysz MA, Gambhir SS, Willmann JK (2010) Molecular imaging: current status and emerging strategies. Clin Radiol 65(7):500–516

5. Kircher MF, Hricak H, Larson SM (2012) Molecular imaging for personalized cancer care. Mol Oncol 6(2):182–195
6. Naumova AV, Modo M, Moore A, Murry CE, Frank JA (2014) Clinical imaging in regenerative medicine. Nat Biotechnol 32(8):804–818
7. Chan KW-Y, Wong W-T (2007) Small molecular gadolinium(III) complexes as MRI contrast agents for diagnostic imaging. Coord Chem Rev 251(17–20):2428–2451
8. Li J, Zheng L, Cai H, Sun W, Shen M, Zhang G, Shi X (2013) Polyethyleneimine-mediated synthesis of folic acid-targeted iron oxide nanoparticles for in vivo tumor MR imaging. Biomaterials 34(33):8382–8392
9. Jin R, Lin B, Li D, Ai H (2014) Superparamagnetic iron oxide nanoparticles for MR imaging and therapy: design considerations and clinical applications. Curr Opin Pharmacol 18:18–27
10. Li L, Gao F, Jiang W, Wu X, Cai Y, Tang J, Gao X, Gao F (2016) Folic acid-conjugated superparamagnetic iron oxide nanoparticles for tumor-targeting MR imaging. Drug Deliv 23 (5):1726–1733
11. Mustafa R, Zhou B, Yang J, Zheng L, Zhang G, Shi X (2016) Dendrimer-functionalized laponite nanodisks loaded with gadolinium for T1-weighted MR imaging applications. RSC Adv 6(97):95112–95119
12. Suzuki H, Oshima H, Shiraki N, Ikeya C, Shibamoto Y (2004) Comparison of two contrast materials with different iodine concentrations in enhancing the density of the aorta, portal vein and liver at multi-detector row CT: a randomized study. Eur Radiol 14(11):2099–2104
13. Hainfeld JF, Slatkin DN, Focella TM, Smilowitz HM (2006) Gold nanoparticles: a new X-ray contrast agent. Br J Radiol 79(939):248–253
14. Popovtzer R, Agrawal A, Kotov NA, Popovtzer A, Balter J, Carey TE, Kopelman R (2008) Targeted gold nanoparticles enable molecular ct imaging of cancer. Nano Lett 8 (12):4593–4596
15. Peng C, Zheng L, Chen Q, Shen M, Guo R, Wang H, Cao X, Zhang G, Shi X (2012) PEGylated dendrimer-entrapped gold nanoparticles for in vivo blood pool and tumor imaging by computed tomography. Biomaterials 33(4):1107–1119
16. Zhang Y, Wen S, Zhao L, Li D, Liu C, Jiang W, Gao X, Gu W, Ma N, Zhao J, Shi X, Zhao Q (2016) Ultrastable polyethyleneimine-stabilized gold nanoparticles modified with polyethylene glycol for blood pool, lymph node and tumor CT imaging. Nanoscale 8(10):5567–5577
17. Ametamey SM, Honer M, Schubiger PA (2008) Molecular imaging with PET. Chem Rev 108 (5):1501–1516
18. Fletcher JW, Djulbegovic B, Soares HP, Siegel BA, Lowe VJ, Lyman GH, Coleman RE, Wahl R, Paschold JC, Avril N, Einhorn LH, Suh WW, Samson D, Delbeke D, Gorman M, Shields AF (2008) Recommendations on the use of 18F-FDG PET in oncology. J Nucl Med 49 (3):480–508
19. Mosconi L, Mistur R, Switalski R, Tsui WH, Glodzik L, Li Y, Pirraglia E, De Santi S, Reisberg B, Wisniewski T, de Leon MJ (2009) FDG-PET changes in brain glucose metabolism from normal cognition to pathologically verified Alzheimer's disease. Eur J Nucl Med Mol Imaging 36(5):811–822
20. Brindle K (2008) New approaches for imaging tumour responses to treatment. Nat Rev Cancer 8(2):94–107
21. Shirani J, Dilsizian V (2011) Nuclear cardiac imaging in hypertrophic cardiomyopathy. J Nucl Cardiol 18(1):123–134
22. Wang G, Stender AS, Sun W, Fang N (2010) Optical imaging of non-fluorescent nanoparticle probes in live cells. Analyst 135(2):215–221
23. Hellebust A, Richards-Kortum R (2012) Advances in molecular imaging: targeted optical contrast agents for cancer diagnostics. Nanomedicine (Lond) 7(3):429–445
24. James ML, Gambhir SS (2012) A molecular imaging primer: modalities, imaging agents, and applications. Physiol Rev 92(2):897–965
25. Cai H, Li K, Shen M, Wen S, Luo Y, Peng C, Zhang G, Shi X (2012) Facile assembly of Fe_3O_4@Au nanocomposite particles for dual mode magnetic resonance and computed tomography imaging applications. J Mater Chem 22(30):15110–15120

26. Herschman HR (2003) Molecular imaging: looking at problems, seeing solutions. Science 302 (5645):605–608
27. Hoffman JM, Gambhir SS (2007) Molecular imaging: the vision and opportunity for radiology in the future. Radiology 244(1):39–47
28. Luo S, Zhang E, Su Y, Cheng T, Shi C (2011) A review of NIR dyes in cancer targeting and imaging. Biomaterials 32(29):7127–7138
29. Beyer T, Townsend DW, Brun T, Kinahan PE, Charron M, Roddy R, Jerin J, Young J, Byars L, Nutt R (2000) A combined PET/CT scanner for clinical oncology. J Nucl Med 41(8):1369–1379
30. Keidar Z, Israel O, Krausz Y (2003) SPECT/CT in tumor imaging: technical aspects and clinical applications. Semin Nucl Med 33(3):205–218
31. Jennings LE, Long NJ (2009) 'Two is better than one'-probes for dual-modality molecular imaging. Chem Commun (24):3511–3524
32. Ogawa M, Regino CAS, Seidel J, Green MV, Xi W, Williams M, Kosaka N, Choyke PL, Kobayashi H (2009) Dual-modality molecular imaging using antibodies labeled with activatable fluorescence and a radionuclide for specific and quantitative targeted cancer detection. Bioconjug Chem 20(11):2177–2184
33. Li K, Wen S, Larson AC, Shen M, Zhang Z, Chen Q, Shi X, Zhang G (2013) Multifunctional dendrimer-based nanoparticles for in vivo MR/CT dual-modal molecular imaging of breast cancer. Int J Nanomedicine 8:2589–2600
34. Chen J, Sun Y, Chen Q, Wang L, Wang S, Tang Y, Shi X, Wang H (2016) Multifunctional gold nanocomposites designed for targeted CT/MR/optical trimodal imaging of human non-small cell lung cancer cells. Nanoscale 8(28):13568–13573
35. Mariani G, Bruselli L, Kuwert T, Kim EE, Flotats A, Israel O, Dondi M, Watanabe N (2010) A review on the clinical uses of SPECT/CT. Eur J Nucl Med Mol Imaging 37(10):1959–1985
36. Thrall MM, DeLoia JA, Gallion H, Avril N (2007) Clinical use of combined positron emission tomography and computed tomography (FDG-PET/CT) in recurrent ovarian cancer. Gynecol Oncol 105(1):17–22
37. Chiti A, Kirienko M, Grégoire V (2010) Clinical use of PET-CT data for radiotherapy planning: what are we looking for? Radiother Oncol 96(3):277–279
38. Delso G, Fürst S, Jakoby B, Ladebeck R, Ganter C, Nekolla SG, Schwaiger M, Ziegler SI (2011) Performance measurements of the Siemens mMR integrated whole-body PET/MR scanner. J Nucl Med 52(12):1914–1922
39. Drzezga A, Souvatzoglou M, Eiber M, Beer AJ, Fürst S, Martinez-Möller A, Nekolla SG, Ziegler S, Ganter C, Rummeny EJ, Schwaiger M (2012) First clinical experience with integrated whole-body PET/MR: comparison to PET/CT in patients with oncologic diagnoses. J Nucl Med 53(6):845–855
40. Liong M, Lu J, Kovochich M, Xia T, Ruehm SG, Nel AE, Tamanoi F, Zink JI (2008) Multifunctional inorganic nanoparticles for imaging, targeting, and drug delivery. ACS Nano 2(5):889–896
41. Rubel C, Hao H, Weibo C (2015) Image-guided drug delivery with single-photon emission computed tomography: a review of literature. Curr Drug Targets 16(6):592–609
42. Guo R, Shi X (2012) Dendrimers in cancer therapeutics and diagnosis. Curr Drug Metab 13 (8):1097–1109
43. Chen X, Gambhir SS, Cheon J (2011) Theranostic nanomedicine. Acc Chem Res 44(10):841
44. Namiki Y, Fuchigami T, Tada N, Kawamura R, Matsunuma S, Kitamoto Y, Nakagawa M (2011) Nanomedicine for cancer: lipid-based nanostructures for drug delivery and monitoring. Acc Chem Res 44(10):1080–1093
45. Lusic H, Grinstaff MW (2013) X-ray-computed tomography contrast agents. Chem Rev 113 (3):1641–1666
46. Mintzer MA, Grinstaff MW (2011) Biomedical applications of dendrimers: a tutorial. Chem Soc Rev 40(1):173–190
47. Sun W, Mignani S, Shen M, Shi X (2016) Dendrimer-based magnetic iron oxide nanoparticles: their synthesis and biomedical applications. Drug Discov Today 21(12):1873–1885

48. Qiao Z, Shi X (2015) Dendrimer-based molecular imaging contrast agents. Prog Polym Sci 44:1–27
49. Tomalia DA, Baker H, Dewald J, Hall M, Kallos G, Martin S, Roeck J, Ryder J, Smith P (1985) A new class of polymers: starburst-dendritic macromolecules. Polym J 17 (1):117–132
50. Bosman AW, Janssen HM, Meijer EW (1999) About dendrimers: structure, physical properties, and applications. Chem Rev 99(7):1665–1688
51. Tomalia DA, Fréchet JMJ (2002) Discovery of dendrimers and dendritic polymers: a brief historical perspective. J Polym Sci Part A Polym Chem 40(16):2719–2728
52. Shen M, Shi X (2010) Dendrimer-based organic/inorganic hybrid nanoparticles in biomedical applications. Nanoscale 2(9):1596–1610
53. Tang J, Sheng Y, Hu H, Shen Y (2013) Macromolecular MRI contrast agents: structures, properties and applications. Prog Polym Sci 38(3–4):462–502
54. Kobayashi H, Brechbiel MW (2005) Nano-sized MRI contrast agents with dendrimer cores. Adv Drug Deliv Rev 57(15):2271–2286
55. Kobayashi H, Kawamoto S, Jo S-K, Bryant HL, Brechbiel MW, Star RA (2003) Macromolecular MRI contrast agents with small dendrimers: pharmacokinetic differences between sizes and cores. Bioconjug Chem 14(2):388–394
56. Hong S, Leroueil PR, Majoros IJ, Orr BG, Baker JR Jr, Banaszak Holl MM (2007) The binding avidity of a nanoparticle-based multivalent targeted drug delivery platform. Chem Biol 14(1):107–115
57. Shukla R, Hill E, Shi X, Kim J, Muniz MC, Sun K, Baker JR (2008) Tumor microvasculature targeting with dendrimer-entrapped gold nanoparticles. Soft Matter 4(11):2160–2163
58. Shi X, Wang S, Sun H, Baker JR (2007) Improved biocompatibility of surface functionalized dendrimer-entrapped gold nanoparticles. Soft Matter 3(1):71–74
59. Cao Y, Liu H, Shi X (2015) Targeted CT imaging of cancer cells using PEGylated low-generation dendrimer-entrapped gold nanoparticles. J Control Release 213:e138–e139
60. Zhou B, Zheng L, Peng C, Li D, Li J, Wen S, Shen M, Zhang G, Shi X (2014) Synthesis and characterization of PEGylated polyethylenimine-entrapped gold nanoparticles for blood pool and tumor CT imaging. ACS Appl Mater Interfaces 6(19):17190–17199
61. Wang H, Zheng L, Peng C, Shen M, Shi X, Zhang G (2013) Folic acid-modified dendrimer-entrapped gold nanoparticles as nanoprobes for targeted CT imaging of human lung adencarcinoma. Biomaterials 34(2):470–480
62. Talanov VS, Regino CAS, Kobayashi H, Bernardo M, Choyke PL, Brechbiel MW (2006) Dendrimer-based nanoprobe for dual modality magnetic resonance and fluorescence imaging. Nano Lett 6(7):1459–1463
63. Kim Y, Kim SH, Tanyeri M, Katzenellenbogen JA, Schroeder CM (2013) Dendrimer probes for enhanced photostability and localization in fluorescence imaging. Biophys J 104 (7):1566–1575
64. Taratula O, Schumann C, Duong T, Taylor KL, Taratula O (2015) Dendrimer-encapsulated naphthalocyanine as a single agent-based theranostic nanoplatform for near-infrared fluorescence imaging and combinatorial anticancer phototherapy. Nanoscale 7(9):3888–3902
65. Bryant LH Jr, Jordan EK, Bulte JWM, Herynek V, Frank JA (2002) Pharmacokinetics of a high-generation dendrimer–Gd-DOTA. Acad Radiol 9(Suppl 1):S29–S33
66. Wen S, Li K, Cai H, Chen Q, Shen M, Huang Y, Peng C, Hou W, Zhu M, Zhang G, Shi X (2013) Multifunctional dendrimer-entrapped gold nanoparticles for dual mode CT/MR imaging applications. Biomaterials 34(5):1570–1580
67. Nwe K, Bernardo M, Regino CAS, Williams M, Brechbiel MW (2010) Comparison of MRI properties between derivatized DTPA and DOTA gadolinium–dendrimer conjugates. Bioorg Med Chem 18(16):5925–5931
68. Luo Y, Zhao L, Li X, Yang J, Guo L, Zhang G, Shen M, Zhao J, Shi X (2016) The design of a multifunctional dendrimer-based nanoplatform for targeted dual mode SPECT/MR imaging of tumors. J Mater Chem B 4(45):7220–7225

69. Li X, Xiong Z, Xu X, Luo Y, Peng C, Shen M, Shi X (2016) 99mTc-labeled multifunctional low-generation dendrimer-entrapped gold nanoparticles for targeted SPECT/CT dual-mode imaging of tumors. ACS Appl Mater Interfaces 8(31):19883–19891
70. Zhao L, Zhu J, Cheng Y, Xiong Z, Tang Y, Guo L, Shi X, Zhao J (2015) Chlorotoxin-conjugated multifunctional dendrimers labeled with radionuclide 131I for single photon emission computed tomography imaging and radiotherapy of gliomas. ACS Appl Mater Interfaces 7(35):19798–19808
71. Seo JW, Baek H, Mahakian LM, Kusunose J, Hamzah J, Ruoslahti E, Ferrara KW (2014) 64Cu-labeled lyp-1-dendrimer for PET-CT imaging of atherosclerotic plaque. Bioconjug Chem 25(2):231–239
72. Ghai A, Singh B, Panwar Hazari P, Schultz MK, Parmar A, Kumar P, Sharma S, Dhawan D, Kumar Mishra A (2015) Radiolabeling optimization and characterization of 68Ga labeled DOTA–polyamido-amine dendrimer conjugate – animal biodistribution and PET imaging results. Appl Radiat Isot 105:40–46
73. Bulte JWM, Douglas T, Witwer B, Zhang S-C, Strable E, Lewis BK, Zywicke H, Miller B, van Gelderen P, Moskowitz BM, Duncan ID, Frank JA (2001) Magnetodendrimers allow endosomal magnetic labeling and in vivo tracking of stem cells. Nat Biotechnol 19(12):1141–1147
74. Strable E, Bulte JWM, Moskowitz B, Vivekanandan K, Allen M, Douglas T (2001) Synthesis and characterization of soluble iron oxide–dendrimer composites. Chem Mater 13 (6):2201–2209
75. Shi X, Thomas TP, Myc LA, Kotlyar A, Baker JJR (2007) Synthesis, characterization, and intracellular uptake of carboxyl-terminated poly(amidoamine) dendrimer-stabilized iron oxide nanoparticles. Phys Chem Chem Phys 9(42):5712–5720
76. Zhou B, Xiong Z, Zhu J, Shen M, Tang G, Peng C, Shi X (2016) PEGylated polyethylenimine-entrapped gold nanoparticles loaded with gadolinium for dual-mode CT/MR imaging applications. Nanomedicine 11(13):1639–1652
77. Chen Q, Wang H, Liu H, Wen S, Peng C, Shen M, Zhang G, Shi X (2015) Multifunctional dendrimer-entrapped gold nanoparticles modified with RGD peptide for targeted computed tomography/magnetic resonance dual-modal imaging of tumors. Anal Chem 87(7):3949–3956
78. Shaw LJ, Iskandrian AE (2004) Prognostic value of gated myocardial perfusion SPECT. J Nucl Cardiol 11(2):171–185
79. Gnanasegaran G, Ballinger JR (2014) Molecular imaging agents for SPECT (and SPECT/CT). Eur J Nucl Med Mol Imaging 41(1):26–35
80. Cutler CS, Hennkens HM, Sisay N, Huclier-Markai S, Jurisson SS (2013) Radiometals for combined imaging and therapy. Chem Rev 113(2):858–883
81. Madsen MT (2007) Recent advances in SPECT imaging. J Nucl Med 48(4):661–673
82. Eckelman WC (2009) Unparalleled contribution of technetium-99m to medicine over 5 decades. J Am Coll Cardiol Img 2(3):364–368
83. Khalil MM, Tremoleda JL, Bayomy TB, Gsell W (2011) Molecular SPECT imaging: an overview. Int J Mol Imaging 2011:796025
84. Niendorf HP, Dinger JC, Haustein J, Cornelius I, Alhassan A, Clauß W (1991) Tolerance data of Gd-DTPA: a review. Eur J Radiol 13(1):15–20
85. Weinmann HJ, Brasch RC, Press WR, Wesbey GE (1984) Characteristics of gadolinium-DTPA complex: a potential NMR contrast agent. Am J Roentgenol 142(3):619–624
86. Brix G, Semmler W, Port R, Schad LR, Layer G, Lorenz WJ (1991) Pharmacokinetic parameters in CNS Gd-DTPA enhanced MR imaging. J Comput Assist Tomogr 15(4):621–628
87. Lorberboym M, Lampl Y, Sadeh M (2003) Correlation of 99mTc-DTPA SPECT of the blood–brain barrier with neurologic outcome after acute stroke. J Nucl Med 44(12):1898–1904
88. McLarty K, Cornelissen B, Cai Z, Scollard DA, Costantini DL, Done SJ, Reilly RM (2009) Micro-SPECT/CT with 111In-DTPA-pertuzumab sensitively detects trastuzumab-mediated her2 downregulation and tumor response in athymic mice bearing MDA-MB-361 human breast cancer xenografts. J Nucl Med 50(8):1340–1348

89. Bar-Shalom R, Yefremov N, Guralnik L, Keidar Z, Engel A, Nitecki S, Israel O (2006) SPECT/CT using 67Ga and 111In-labeled leukocyte scintigraphy for diagnosis of infection. J Nucl Med 47(4):587–594
90. Zhang Y, Sun Y, Xu X, Zhu H, Huang L, Zhang X, Qi Y, Shen Y-M (2010) Radiosynthesis and micro-SPECT imaging of 99mTc-dendrimer poly(amido)-amine folic acid conjugate. Bioorg Med Chem Lett 20(3):927–931
91. Zhang Y, Sun Y, Xu X, Zhang X, Zhu H, Huang L, Qi Y, Shen Y-M (2010) Synthesis, biodistribution, and microsingle photon emission computed tomography (SPECT) imaging study of technetium-99m labeled pegylated dendrimer poly(amidoamine) (PAMAM)−folic acid conjugates. J Med Chem 53(8):3262–3272
92. Xu X, Zhang Y, Wang X, Guo X, Zhang X, Qi Y, Shen Y-M (2011) Radiosynthesis, biodistribution and micro-SPECT imaging study of dendrimer–avidin conjugate. Bioorg Med Chem 19(5):1643–1648
93. Mirzaii M, Seyyedi S, Sadeghi M, Gholamzadeh Z (2010) Cadmium electrodeposition on copper substrate for cyclotron production of 111In radionuclide. J Radioanal Nucl Chem 284 (2):333–339
94. Mamede M, Saga T, Ishimori T, Higashi T, Sato N, Kobayashi H, Brechbiel MW, Konishi J (2004) Hepatocyte targeting of 111In-labeled oligo-DNA with avidin or avidin–dendrimer complex. J Control Release 95(1):133–141
95. Bindslev L, Haack-Sørensen M, Bisgaard K, Kragh L, Mortensen S, Hesse B, Kjær A, Kastrup J (2006) Labelling of human mesenchymal stem cells with indium-111 for SPECT imaging: effect on cell proliferation and differentiation. Eur J Nucl Med Mol Imaging 33(10):1171–1177
96. Wong KK, Cahill JM, Frey KA, Avram AM (2010) Incremental value of 111-in pentetreotide SPECT/CT fusion imaging of neuroendocrine tumors. Acad Radiol 17(3):291–297
97. Castaldi P, Rufini V, Treglia G, Bruno I, Perotti G, Stifano G, Barbaro B, Giordano A (2008) Impact of 111In-DTPA-octreotide SPECT/CT fusion images in the management of neuroendocrine tumours. Radiol Med 113(7):1056–1067
98. Kojima C, Niki Y, Ogawa M, Magata Y (2014) Prolonged local retention of subcutaneously injected polymers monitored by noninvasive SPECT imaging. Int J Pharm 476(1–2):164–168
99. Keshtgar MRS, Ell PJ (1999) Sentinel lymph node detection and imaging. Eur J Nucl Med 26 (1):57–67
100. Xie Y, Bagby TR, Cohen MS, Forrest ML (2009) Drug delivery to the lymphatic system: importance in future cancer diagnosis and therapies. Expert Opin Drug Deliv 6(8):785–792
101. Ryan GM, Kaminskas LM, Porter CJH (2014) Nano-chemotherapeutics: maximising lymphatic drug exposure to improve the treatment of lymph-metastatic cancers. J Control Release 193:241–256
102. Koyama Y, Talanov VS, Bernardo M, Hama Y, Regino CAS, Brechbiel MW, Choyke PL, Kobayashi H (2007) A dendrimer-based nanosized contrast agent dual-labeled for magnetic resonance and optical fluorescence imaging to localize the sentinel lymph node in mice. J Magn Reson Imaging 25(4):866–871
103. Jain R, Dandekar P, Patravale V (2009) Diagnostic nanocarriers for sentinel lymph node imaging. J Control Release 138(2):90–102
104. Sano K, Iwamiya Y, Kurosaki T, Ogawa M, Magata Y, Sasaki H, Ohshima T, Maeda M, Mukai T (2014) Radiolabeled γ-polyglutamic acid complex as a nano-platform for sentinel lymph node imaging. J Control Release 194:310–315
105. Niki Y, Ogawa M, Makiura R, Magata Y, Kojima C (2015) Optimization of dendrimer structure for sentinel lymph node imaging: effects of generation and terminal group. Nanomedicine 11(8):2119–2127
106. Willi AK (2006) X-ray computed tomography. Phys Med Biol 51(13):R29
107. Mattrey RF, Aguirre DA (2003) Advances in contrast media research. Acad Radiol 10 (12):1450–1460
108. Hallouard F, Anton N, Choquet P, Constantinesco A, Vandamme T (2010) Iodinated blood pool contrast media for preclinical X-ray imaging applications – a review. Biomaterials 31 (24):6249–6268

109. Liu H, Wang H, Xu Y, Shen M, Zhao J, Zhang G, Shi X (2014) Synthesis of PEGylated low generation dendrimer-entrapped gold nanoparticles for CT imaging applications. Nanoscale 6 (9):4521–4526
110. Wang H, Zheng L, Guo R, Peng C, Shen M, Shi X, Zhang G (2012) Dendrimer-entrapped gold nanoparticles as potential CT contrast agents for blood pool imaging. Nanoscale Res Lett 7 (1):190
111. Peng C, Qin J, Zhou B, Chen Q, Shen M, Zhu M, Lu X, Shi X (2013) Targeted tumor CT imaging using folic acid-modified PEGylated dendrimer-entrapped gold nanoparticles. Polym Chem 4(16):4412–4424
112. Criscione JM, Dobrucki LW, Zhuang ZW, Papademetris X, Simons M, Sinusas AJ, Fahmy TM (2011) Development and application of a multimodal contrast agent for SPECT/CT hybrid imaging. Bioconjug Chem 22(9):1784–1792
113. Xu C, Tung GA, Sun S (2008) Size and concentration effect of gold nanoparticles on X-ray attenuation as measured on computed tomography. Chem Mater 20(13):4167–4169
114. Shi X, Lee I, Baker JR (2008) Acetylation of dendrimer-entrapped gold and silver nanoparticles. J Mater Chem 18(5):586–593
115. Guo R, Wang H, Peng C, Shen M, Pan M, Cao X, Zhang G, Shi X (2010) X-ray attenuation property of dendrimer-entrapped gold nanoparticles. J Phys Chem C 114(1):50–56
116. Jordan LC, McKinstry RC, Kraut MA, Ball WS, Vendt BA, Casella JF, DeBaun MR, Strouse JJ (2010) Incidental findings on brain magnetic resonance imaging of children with sickle cell disease. Pediatrics 126(1):53
117. Beets-Tan RGH, Beets GL (2004) Rectal cancer: review with emphasis on MR imaging. Radiology 232(2):335–346
118. Raymond KN, Pierre VC (2005) Next generation, high relaxivity gadolinium MRI agents. Bioconjug Chem 16(1):3–8
119. Yang C-T, Chuang K-H (2012) Gd(iii) chelates for MRI contrast agents: from high relaxivity to "smart", from blood pool to blood-brain barrier permeable. Med Chem Commun 3 (5):552–565
120. Cheng C-Y, Ou K-L, Huang W-T, Chen J-K, Chang J-Y, Yang C-H (2013) Gadolinium-based CuInS2/ZnS nanoprobe for dual-modality magnetic resonance/optical imaging. ACS Appl Mater Interfaces 5(10):4389–4400
121. Langereis S, de Lussanet QG, van Genderen MHP, Meijer EW, Beets-Tan RGH, Griffioen AW, van Engelshoven JMA, Backes WH (2006) Evaluation of Gd(III)DTPA-terminated poly (propylene imine) dendrimers as contrast agents for MR imaging. NMR Biomed 19 (1):133–141
122. Cheng Z, Thorek DLJ, Tsourkas A (2010) Gadolinium-conjugated dendrimer nanoclusters as a tumor-targeted T1 magnetic resonance imaging contrast agent. Angew Chem Int Ed Engl 49 (2):346–350
123. Rahmania H, Mutalib A, Ramli M, Levita J (2015) Synthesis and stability test of radiogadolinium(III)-DOTA-PAMAM G3.0-trastuzumab as SPECT-MRI molecular imaging agent for diagnosis of HER-2 positive breast cancer. J Radiat Res Appl Sci 8(1):91–99
124. Lee WI, Bae Y, Bard AJ (2004) Strong blue photoluminescence and ECL from OH-terminated PAMAM dendrimers in the absence of gold nanoparticles. J Am Chem Soc 126 (27):8358–8359
125. Wang D, Imae T (2004) Fluorescence emission from dendrimers and its pH dependence. J Am Chem Soc 126(41):13204–13205
126. Tsuchimochi M, Hayama K, Toyama M, Sasagawa I, Tsubokawa N (2013) Dual-modality imaging with 99mTc and fluorescent indocyanine green using surface-modified silica nanoparticles for biopsy of the sentinel lymph node: an animal study. EJNMMI Res 3(1):33
127. Xie J, Lee S, Chen X (2010) Nanoparticle-based theranostic agents. Adv Drug Deliv Rev 62 (11):1064–1079
128. Ma Y, Mou Q, Wang D, Zhu X, Yan D (2016) Dendritic polymers for theranostics. Theranostics 6(7):930–947

129. Zhu J, Zhao L, Cheng Y, Xiong Z, Tang Y, Shen M, Zhao J, Shi X (2015) Radionuclide 131I-labeled multifunctional dendrimers for targeted SPECT imaging and radiotherapy of tumors. Nanoscale 7(43):18169–18178
130. Cheng Y, Zhu J, Zhao L, Xiong Z, Tang Y, Liu C, Guo L, Qiao W, Shi X, Zhao J (2016) 131I-labeled multifunctional dendrimers modified with BmK CT for targeted SPECT imaging and radiotherapy of gliomas. Nanomedicine 11(10):1253–1266
131. Vugmeyster Y, DeFranco D, Szklut P, Wang Q, Xu X (2010) Biodistribution of [125I]-labeled therapeutic proteins: application in protein drug development beyond oncology. J Pharm Sci 99(2):1028–1045
132. Shao X, Zhang H, Rajian JR, Chamberland DL, Sherman PS, Quesada CA, Koch AE, Kotov NA, Wang X (2011) 125I-labeled gold nanorods for targeted imaging of inflammation. ACS Nano 5(11):8967–8973
133. Merkel OM, Mintzer MA, Sitterberg J, Bakowsky U, Simanek EE, Kissel T (2009) Triazine dendrimers as nonviral gene delivery systems: effects of molecular structure on biological activity. Bioconjug Chem 20(9):1799–1806
134. Mintzer MA, Merkel OM, Kissel T, Simanek EE (2009) Polycationic triazine-based dendrimers: effect of peripheral groups on transfection efficiency. New J Chem 33 (9):1918–1925
135. Merkel OM, Zheng M, Mintzer MA, Pavan GM, Librizzi D, Maly M, Höffken H, Danani A, Simanek EE, Kissel T (2011) Molecular modeling and in vivo imaging can identify successful flexible triazine dendrimer-based siRNA delivery systems. J Control Release 153(1):23–33
136. Lee C, Lo S-T, Lim J, da Costa VCP, Ramezani S, Öz OK, Pavan GM, Annunziata O, Sun X, Simanek EE (2013) Design, synthesis and biological assessment of a triazine dendrimer with approximately 16 paclitaxel groups and 8 PEG groups. Mol Pharm 10(12):4452–4461
137. Xiao W, Luo J, Jain T, Riggs JW, Tseng HP, Henderson PT, Cherry SR, Rowland D, Lam KS (2012) Biodistribution and pharmacokinetics of a telodendrimer micellar paclitaxel nanoformulation in a mouse xenograft model of ovarian cancer. Int J Nanomedicine 7 (9):1587–1597